Evolution of helium bubbles in aluminum during heavy-ion irradiation

R. C. Birtcher
Materials Science Department, Argonne National Laboratory, Argonne, Illinois 60439

S. E. Donnelly
Department of Electronic and Electrical Engineering, University of Salford, Salford M5 4WT, United Kingdom

C. Templier
Laboratoire de Métallurgie Physique, Université de Poitiers, 40 avenue du Recteur Pineau, 86022 Poitiers Cédex, France
(Received 14 February 1994)

The evolution of individual He bubbles in thin Al foils during 200-keV Xe irradiation at room-temperature has been followed with *in situ* transmission electron microscopy. He bubbles were produced by room-temperature implantation of 3-keV He ions into prethinned aluminum samples. During subsequent xenon irradiation, several distinct processes were observed to cause individual He bubbles to increase or decrease in size. Bubble growth was observed to take place by radiation-induced coalescence of bubbles without bubble motion. This coalescence was a result of the net displacement of Al atoms out of the volume between bubbles initially in close proximity. The resulting nonequilibrium-shaped bubble evolved towards a more energetically favorable spherical shape whose final size was determined by equilibrium bubble pressure. Bubbles were observed to disappear as the specimen surface was removed by sputtering. Bubbles unaffected by sputtering were observed to decrease in size at an average rate of 0.1 to 0.2 nm/(10^{15} Xe/cm^2) or 0.024 to 0.048 nm/dpa (displacements per atom). This rate of bubble shrinkage can be understood on the basis of direct displacement of He out of the bubble while the bubble remains at equilibrium pressure. He resolution occurred at a rate of 0.005 to 0.01 ($He^{ejected}$/He)/dpa. No examples were found that would indicate complete destruction of a bubble by a single Xe ion. Bubble centers remained fixed during bubble shrinkage indicating negligible bubble motion during room-temperature irradiation.

INTRODUCTION

Research into the behavior of inert gases energetically implanted into a variety of solid materials has been carried out over the last 40 years driven primarily by technological questions associated with the behavior of materials in nuclear reactor environments.[1] Interest in the behavior of helium arises out of possible problems with the integrity of the first wall of the proposed controlled thermonuclear reactor and helium embrittlement in nuclear reactors. Studies of helium in elemental materials provides insights into fundamental behavior of relevance to more complex systems such as heavy inert gases in nuclear fuels and in the engineering materials from which reactors are constructed. Despite the apparent simplicity of a system consisting only of an elemental metal and implanted helium, a number of interesting phenomena have been observed in previous work. These include small bubbles containing helium at pressures of tens of thousands of atmospheres or greater,[2-5] helium bubble superlattices,[6] and helium platelets.[7] However, despite more than four decades of research, important questions remain unclear or unanswered about helium behavior in metals.

Of particular interest from a technological viewpoint is the behavior of gas bubbles in the complex environment of a reactor where both high temperatures and damaging irradiation have important influences on bubble kinetics. A significant body of literature exists on the thermal behavior of helium bubbles including both implantation into heated substrates and post-irradiation annealing,[8,9] but only scant information is available on the behavior of bubbles under irradiation and none from direct observations. Based on microscopic observations of mean bubble sizes in reactor fuels, mechanisms such as bubble dissolution by a single fission fragment and He resolution have been proposed.[10] The details of these mechanisms are subject of interpretation and modeling, and the parameters describing He resolution vary over many orders of magnitude. The present manuscript reports observations of the evolution of helium bubbles in aluminum during irradiation with 200-keV Xe ions. The study utilized an *in situ* ion irradiation facility that allows the evolution of individual bubbles to be followed in detail by transmission electron microscopy.

EXPERIMENT

Specimens were prepared from polycrystalline Al (99.9999 at. % pure) with grain size greater than 10 μm 3-mm disks were thinned by jet polishing in a solution of 28% HNO_3, 65% methanol, and 7% butyl cellosolve at -45 °C. Thinned specimens were subsequently implanted, at room temperature, with 3-keV helium ions to a dose of 10^{17} He/cm^2 using an ion gun mounted on a small turbo-pumped vacuum chamber that achieved a base pressure of $\approx 10^{-7}$ mbar. Although the ion beam was not mass filtered, consideration of the base and helium

pressures in various parts of the gun indicates that impurities constitute less than 0.05% of the ion beam. Implantation was carried out at a flux of 6×10^{13} He/cm^2 s ($\approx$30 mW/cm^2) giving rise to negligible heating of the specimen. Room-temperature Xe irradiations and *in situ* observations were performed at the HVEM-Accelerator Facility located at Argonne National Laboratory.[11] This facility consists of a modified Kratos/AE1 EM7 high-voltage electron microscope (HVEM) and a 0.6-MV National Electrostatics ion accelerator. Specimens were irradiated with the ion beam incident 10° away from the surface normal at a dose rate of 1.7×10^{12} Xe/cm^2 s. The highest temperature increase produced by beam heating during Xe irradiation was estimated to be less than 10 °C. The electron energy in the HVEM was maintained at 200 kV to minimize displacement damage from electron irradiation, and TEM images were made with the ion beam off. Specimen transfers between the different facilities were made in air.

Monte Carlo calculations, using TRIM 91 (Ref. 12) indicate that the peak in the range of 3-keV He in Al is at a depth of 37 nm with a straggling of 19 nm. Similar calculations for 200-keV Xe (range 77 nm, straggling 17 nm) indicate that the displacement damage extends over the entire range profile of the helium with an average damage rate of 4.2 dpa/(10^{15}Xe/cm^2) in pure Al. Less than 12% of the Xe was stopped in the specimen (estimated to be 50 nm thick) resulting in a peak Xe concentration of 0.6% at the end of the Xe irradiation.

RESULTS AND DISCUSSION

Helium bubble evolution in a thin specimen during 200-keV Xe irradiation at room temperature is shown in Fig. 1 by a series of TEM micrographs taken after irradi-

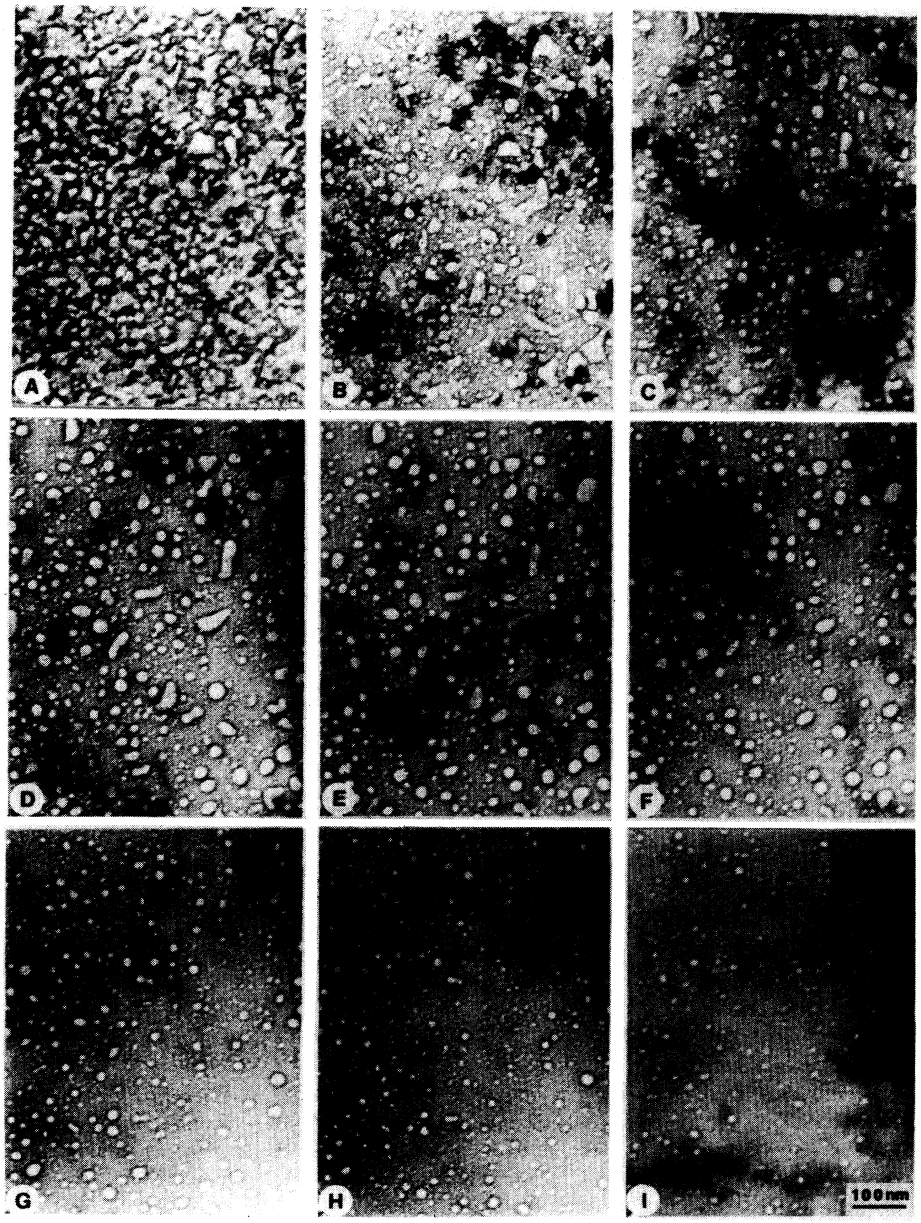

FIG. 1. TEM micrographs showing He bubble evolution during 200-keV Xe irradiation at room temperature. Xe dose of (a) 0, (b) 2, (c) 4, (d) 6, (e) 8, (f) 10, (g) 12, (h) 13, and (i) 15×10^{15} Xe/cm^2.

ation to increasing doses. Images were recorded after dose increments of 10^{15} Xe/cm^2, and only a selection is shown in Fig. 1. The most obvious feature in the microstructure after He implantation consists of large irregular bubbles which are associated with the surface oxide on the Al. In addition, there are smaller spherical bubbles within the Al. This is consistent with other work on He implantation at room temperature into Al.[2] The surface oxide and large bubbles associated with the surface oxide were removed by atomic sputtering of the specimen after a dose of $\approx 3\times 10^{15}$ Xe/cm^2. A sputtering yield of 10 (Ref. 13) implies that the oxide layer was approximately 5 nm thick, consistent with expectations of the thickness of the oxide layer found on Al exposed to air. At doses above 3×10^{15} Xe/cm^2, the evolution of existing individual He bubbles within the Al could be easily followed. No additional bubbles were observed to nucleate.

The physics of He bubble behavior during irradiation is displayed by those bubbles remaining after the surface layer was removed. The bubbles in Fig. 1 undergo drastic changes in morphology during the Xe irradiation due to both growth by coalescence and shrinkage. Coalescence of two bubbles produces a larger, irregular bubble that tends to become spherical (circular in the TEM image) during continued Xe irradiation. Bubbles decrease in size at two different rates due to two different processes. Some bubbles disappear quickly over a limited dose range while others slowly reduce in size. The details of each of these processes will be discussed in the following sections. Triangulation measurements of bubbles separated by more than 1 μm shows that bubbles do not undergo changes in position because of irradiation induced or enhanced diffusion. Brownian motion of Xe bubbles in Al has been observed during *in situ* irradiation with Al ions at temperatures between 400 and 500 °C.[14] Extrapolation of these results to room temperature is consistent with the inability to discern He bubble motion during this room temperature Xe irradiation.

An example of a typical bubble coalescence event is marked in Fig. 1(d) in an area where three bubbles were initially located in close proximity. At a dose of 7×10^{15} Xe/cm^2, two of the three bubbles coalesced. Subsequently the two remaining bubbles coalesce at a dose of 10×10^{15} Xe/cm^2. After both coalescence events, the resultant enlarged irregular-shaped bubble "rounded out" to a circular shape in the TEM image which we assume indicates a spherical bubble. Evolution towards a spherical shape would reduce the total energy by removing variations in the local radius of curvature and decreasing total bubble surface area. In all cases, coalescence occurred over a finite dose range and did not appear to result from a single Xe ion impact. Detailed examination of the TEM micrographs indicates that the process of coalescence involved gradual erosion of the material between the bubbles. It should be emphasized that this behavior was observed for all coalescence events of which the group of bubbles marked in Fig. 1 is a representative example.

Bubble coalescence without bubble motion can be understood on the basis of a difference in the probability for an Al atom to be knocked out of the volume between a pair of bubbles and the probability for an Al atom to be injected into this interbubble volume. Based on TRIM calculations, 200-keV Xe ions displace Al in our specimen at a rate of 4.2 Al dpa/(10^{15} Xe/cm^2), and approximately $\frac{1}{3}$ of the Al recoils receive sufficient energy to travel distances on the order of the distance between coalescencing bubbles (~ 100 Å). This leads to an Al flux out of the interbubble volume of approximately 1.4 Al dpa/(10^{15} Xe/cm^2). If the bubbles contained Al, this would also be the rate of Al displacement into the interbubble volume and the net flux of Al atoms would be zero. However since an Al flux cannot come from bubble volumes, the flux of Al into the interbubble volume is reduced by the bubble volume fraction of approximately 0.1. The net Al flux is approximately the difference in fluxes or 0.14 Al dpa/(10^{15} Xe/cm^2), leading to disappearance of the 100-Å-thick interbubble volume after 7×10^{15} Xe/cm^2. This calculation provides only an estimate, and the actual rate would increase as the interbubble volume between bubbles became thinner due to a larger fraction of Al recoils having sufficient energy to escape. Our observations indicate that such coalescence required between 5 and 10×10^{15} Xe/cm^2 depending on the distance between bubbles.

Evolution of the radii of the three bubbles shown in Fig. 1 with Xe dose is shown in Fig. 2(a). Shown in Fig. 2(b) are the radii equivalent to a single bubble with the same total volume contained in the three bubbles as well

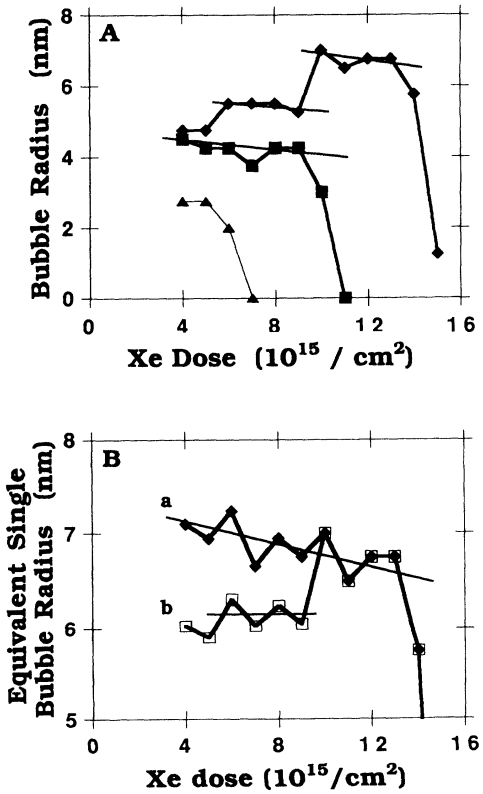

FIG. 2. Changes in three bubbles indicated in Fig. 1 during coalescence: (a) radii of three bubbles as a function of Xe dose, and (b) radii of a single bubble equivalent to (*a*) total surface area of the three bubbles and (*b*) total volume of the three bubbles as a function of Xe dose.

as that for a single bubble with the same total surface area as the three bubbles, assuming that the bubbles are spherical. The increase in total bubble volume after coalescence indicates that during subsequent Xe irradiation the bubble pressure decreased, i.e., the He density was lowered for the same number of He atoms. If bubbles did not increase in size after coalescence, their pressure would increase, and they would become over pressurized. This jump in bubble volume suggests that bubbles acquire through irradiation the necessary vacancies so that, for the total number of He atoms involved, the bubbles are at or near equilibrium pressures during the entire Xe irradiation. This is possible because of the flux of defects produced by the Xe irradiation which results in the generation of ≈ 4.2 dpa for each 10^{15} Xe/cm^2 dose increment incident on the specimen. In other works, He bubbles have been assumed to be at equilibrium pressure after vacancy generation by thermal annealing.[3,15]

From Fig. 2 it can be seen that within our resolution the total bubble surface area is unaffected by bubble coalescence. To understand the implication of this observation, we assume that helium in these bubbles behaves as an ideal gas. Bubbles at equilibrium are expected to have a pressure, P, related to their radius, r, and free surface energy, γ, by $P=2\gamma/r$.[2,3,15] Under these assumptions, the total bubble surface area, i.e., the sum of the squares of the bubble radii, will be conserved after coalescence when all gas atoms are in a single bubble. In atomistic terms, after a coalescence event the new bubble is over pressurized but quickly relaxes to the equilibrium pressure by an increase in volume. The overall gradual decrease of the total bubble size in Fig. 2 with Xe dose is due to helium resolution from the bubble, and the details of this process will be discussed below. The rapid size decrease of the final bubble at doses above 13×10^{15} Xe/cm^2 is due to sputtering of the Al surface and will be discussed next. All cases of bubble growth investigated in such detail were found to be due to coalescence events.

The decrease of bubble size during Xe irradiation evident in Fig. 1 exhibits two different types of behavior. Many bubbles exhibit a slow decrease in size while some bubbles undergo a rapid decrease and disappear over a narrow dose range. The dose dependences of the radius for three bubbles with different radii displaying the second type of behavior are shown in Fig. 3. Bubble growth evident in Fig. 3 was determined as being due to coalescence with other bubbles initially in close proximity to the bubble under observation and exhibited the same conservation of total bubble surface area discussed above and displayed in Fig. 2. For these rapidly shrinking bubbles, the radius decreased at a rate between 1.2 and 2.5 nm/(10^{15} Xe/cm^2). The rapid bubble shrinkage to the point of disappearance was due to erosion of the specimen surface by sputtering. Bubble shrinkage in the TEM image is assumed to be due to a change in the image contrast that began when the surface was eroded to the point of contacting the bubble and ended when the surface reached the bubble center reducing the bubble to surface roughness. The rapid shrinkage rates corresponds to a sputtering yield between 7 and 15 consistent with the expected value of 10.[13] The largest bubble in Fig. 3 extend-

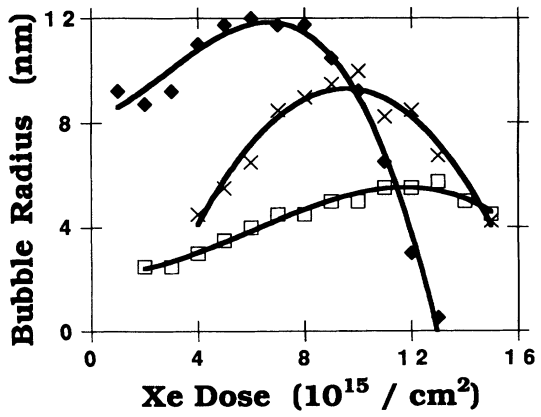

FIG. 3. Changes in individual bubbles undergoing growth by coalescence followed by shrinkage due to surface sputtering during Xe irradiation at room temperature.

ed closer to the specimen surface and thus disappeared at a lower Xe dose. The largest bubble in Fig. 3 began to disappear after a dose of 10×10^{15} Xe/cm^2. A sputtering yield of 10 implies that the center of this 12-nm radius bubble was (17+12=)29 nm below the specimen surface. The centers of the other two bubbles shown in Fig. 3 are estimated to lie at depths of 29 and 30.5 nm. Calculations indicate that bubbles exhibiting rapid shrinkage are centered within the peak in the calculated range of the implanted He. As was mentioned above, sputtering was also responsible for the dramatic change in bubble morphology during the initial 3×10^{15} Xe/cm^2 of irradiation when very large bubbles under the surface oxide were removed.

Figure 4 displays a bubble shrinkage behavior that involves a fundamental process. For the Xe dose range studied, these bubbles did not undergo the rapid decrease in size due to surface sputtering found for the bubbles in Fig. 3 indicating that these bubbles were deeper in the specimen nearer the end of the range of the implanted He. In this region, the He concentration was less than at the peak of the implant, and the resultant larger bubble separations and lack of bubble mobility during the room-temperature Xe irradiation mitigated bubble coalescence. The radii of these bubbles shrink at rates between 0.1 and

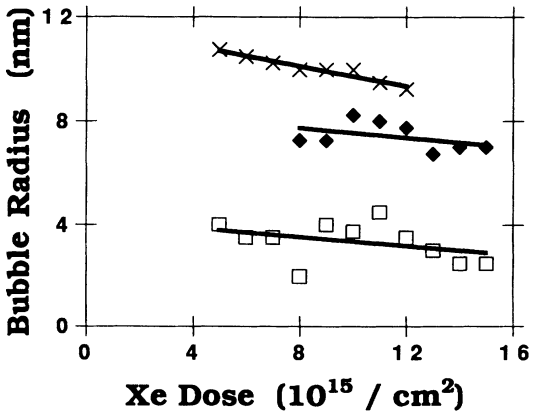

FIG. 4. Changes in individual bubbles undergoing shrinkage due to He resolution during Xe irradiation at room temperature.

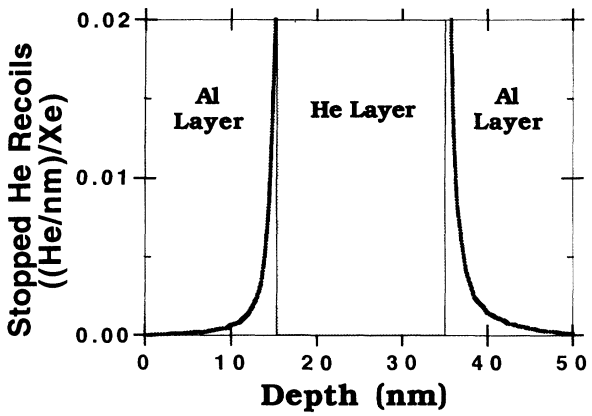

FIG. 5. Results of TRIM calculations of stopping of He ejected from a 20-nm-thick He layer containing 2.5×10^{21} He/cm^3 sandwiched between 15-nm-thick layers of Al. 200-keV Xe ions were incident from the left.

0.2 nm/(10^{15} Xe/cm^2) which is about a tenth of the rate of bubbles that disappear as a result of specimen sputtering. The slow shrinkage of He bubbles is due to a combination of He resolution by the Xe irradiation and Al interstitial absorption. The observed shrinkage rates implies a resolution rate, $(1/n)(dn/d\phi)$, between 0.02 and $(He^{ejected}/He)/(10^{15}$ Xe/cm$^2)$ or 0.005 to 0.01 $(He^{ejected}/He)$/dpa. No examples were found that would indicate complete destruction of a bubble by a single Xe ion.

In order to obtain a qualitative understanding of the effects of Xe irradiation on helium bubbles in aluminum, the system was simulated using TRIM (Ref. 12) with a 20-nm-thick He "bubble" layer containing a density of 2.5×10^{21} He/cm^3 sandwiched between 15-nm-thick Al layers containing dispersed He. The density of He in the bubble layer was taken as the equilibrium density for a spherical bubble 20 nm in diameter.[3] The calculations indicate that most (93%) He and Al displacements result from Al recoils and not from the primary Xe ions. The results depend only slightly on the location of the He layer in the sandwich. He recoils result in the transport of He both from the He layer into the Al layers and from He dispersed in the Al matrix into the He layer. This has the overall effect of reducing the initial difference in helium concentrations between the bubble layer and the Al matrix. This tendency to homogenize the He concentration leads to a resolution of He out of the bubble back into the Al matrix. The stopping positions of He recoils exiting from both sides of the He layer is shown in Fig. 5. The rate of He ejection by more than 0.5 nm from the He layer is 4.1 He/Xe. He ejection from the He layer is offset by He injection in an amount that is proportional to the He concentration in the Al. Calculations indicate that for a He concentration of 12 at. % in the Al,[2] the rate of He injection is 1.5 He/Xe. Thus, the net He flux is 2.6 He/Xe, and during each irradiation step the fractional rate is 0.05 $(He^{ejected}/He)/(10^{15}$ Xe/cm$^2)$. This estimate is only approximate since it depends on a knowledge of the He concentrations in the bubble and dispersed in the Al matrix. Loss of He from the layer is accompanied by injection and stopping of Al atoms in the He layer at a rate of 7.7 Al/Xe which is approximately equal to the sputtering yield of 10 Al/Xe.[13] These atomic fluxes result in bubble shrinkage. This TRIM calculation is one dimensional and does not fully represent a three-dimensional He bubble. Graphic displays of He recoils indicate that a very significant number of He recoils that would escape from a three-dimensional He bubble remain in the He layer because of its infinite extent in the plane normal to the incident Xe-ion flux. However, this is equivalent in a real specimen to He entering a bubble after ejection from distant bubbles. The calculation also neglects kinetic effects due to bubble pressure or interactions between mobile He (or defects) with a bubble. The calculation indicates the magnitude of He resolution and that combined He and Al displacements tend to homogenize the He distribution leading to bubble shrinkage.

The second type of bubble shrinkage observed in this work is driven by the displacement of He atoms out of the bubble into the Al matrix. All bubbles undergo this process as long as they are within the Al foil and contain a He density greater than the surrounding matrix. The rate of shrinkage would be reduced by return of He atoms ejected into positions close to the bubble. The net loss of He from a bubble would result in an underpressure condition unless the bubble shrinks. Bubble shrinkage in response to He resolution and growth of bubbles after coalescence imply that defect fluxes produced during the Xe irradiation maintain the He bubbles at equilibrium pressures. Under the assumptions of ideal-gas behavior and equilibrium bubble pressure, the square of the bubble radius is proportional to the number of He atoms in the bubble, and the rate of change of the bubble radius is given by $dr/d\phi=(r/2n)(dn/d\phi)$, where n is the number of He atoms in the bubble. Assuming that the rate of He loss from a 20-nm-diam-bubble is the one-dimensional rate calculated by TRIM, the rate of change of the bubble radius would be 0.26 nm/(10^{15} Xe/cm^2). Within the limitations of the calculation, this is consistent with the observed shrinkage rates of between 0.1 and 0.2 nm/(10^{15} Xe/cm^2). The observed shrinkage rates implies a resolution rate, $(1/n)(dn/d\phi)$, between 0.02 and 0.04 $(He^{ejected}/He)/(10^{15}$ Xe/cm$^2)$ or 0.005–0.01 $(He^{ejected}/He)$/dpa.

CONCLUSIONS

In situ observations have facilitated identification of a variety of processes involved in the evolution of He bubbles within Al in response to cascade damage produced by irradiation with Xe ions at room temperature. He resolution from a bubble into the matrix is the fundamental driving force responsible for bubble shrinkage. Erosion of the Al matrix between adjacent bubbles results in bubble coalescence without bubble motion. No examples were found that would indicate complete destruction of a bubble by a single Xe ion. Size changes during shrinkage or after coalescence indicate that bubbles remain at equilibrium pressures. TRIM calculations are consistent with both the observed He resolution rate and ion doses required for bubble coalescence.

ACKNOWLEDGMENTS

We would like to thank B. Kestel for specimen preparation, V. Vishnyakov for help with the He implantations, P. Grundy and C. Faunce for provision of the TEM facilities at the University of Salford, and E. Ryan, L. Funk, and S. Ockers of the Electron Microscopy Center at Argonne National Laboratory for their assistance. This work was supported by a collaborative research grant (No. 910670) from NATO and the U.S. DOE-BES Contract No. W-31-109-ENG-38. Laboratoire de Mètallurgie Physique is Laboratoire Associée au CNRS No. 131.

[1] *NATO Advanced Research Workshop on Fundamental Aspects of Inert Gases in Solids,* Vol. 279 of *NATO Advanced Study Institute, Series B: Physics,* edited by S. E. Donnelly and J. H. Evans (Bonas, France, 1990).

[2] S. E. Donnelly, J. C. Rife, J. M. Gilles, and A. A. Lucas, J. Nucl. Mater. **93&94**, 767 (1980).

[3] W. Jäger, R. Manzke, H. Trinkaus, R. Zeller, J. Fink, and G. Crecelius, Radiat. Eff. **78**, 315 (1983).

[4] S. E. Donnelly, A. A. Lucus, J. P. Vigneron, and J. C. Rife, Radiat. Eff. **78**, 337 (1983).

[5] S. E. Donnelly, Radiat. Eff. **90**, 1 (1985).

[6] K. Krishan, Radiat. Eff. **66**, 121 (1982).

[7] A. van Veen, L. M. Casper, and J. H. Evans, J. Nucl. Mater. **104**, 1181 (1981).

[8] K. Ono, M. Inoue, T. Kino, S. Furuno, and K. Izui, J. Nucl. Mater. **133&134**, 477 (1985).

[9] K. Ono, S. Furuno, K. Hojou, T. Kino, K. Izui, O. Takaoka, N. Kubo, K. Mizuno, and K. Ito, J. Nucl. Mater. **191-194**, 1269 (1992).

[10] C. C. Dollins and H. Ocken, J. Nucl. Mater. **45**, 150 (1972).

[11] A. Taylor, C. W. Allen, and E. A. Ryan, Nucl. Instrum. Methods **B24/25**, 598 (1987).

[12] J. F. Ziegler, J. P. Biersack, and U. Littmark, *The Stopping and Ranges of Ions in Solids* (Pergamon, New York, 1985).

[13] H. H. Anderson and H. L. Bay, *Topics in Applied Physics,* Vol. 47, edited by R. Behrisch (Springer-Verlag, Berlin, 1981), p. 145.

[14] D. E. Alexander and R. C. Birtcher, J. Nucl. Mater. **191-194**, 1289 (1992).

[15] H. Trinkhaus, *Nato Advanced Research Workshop on Fundamental Aspects of Inert Cases in Solids* (Ref. 1).

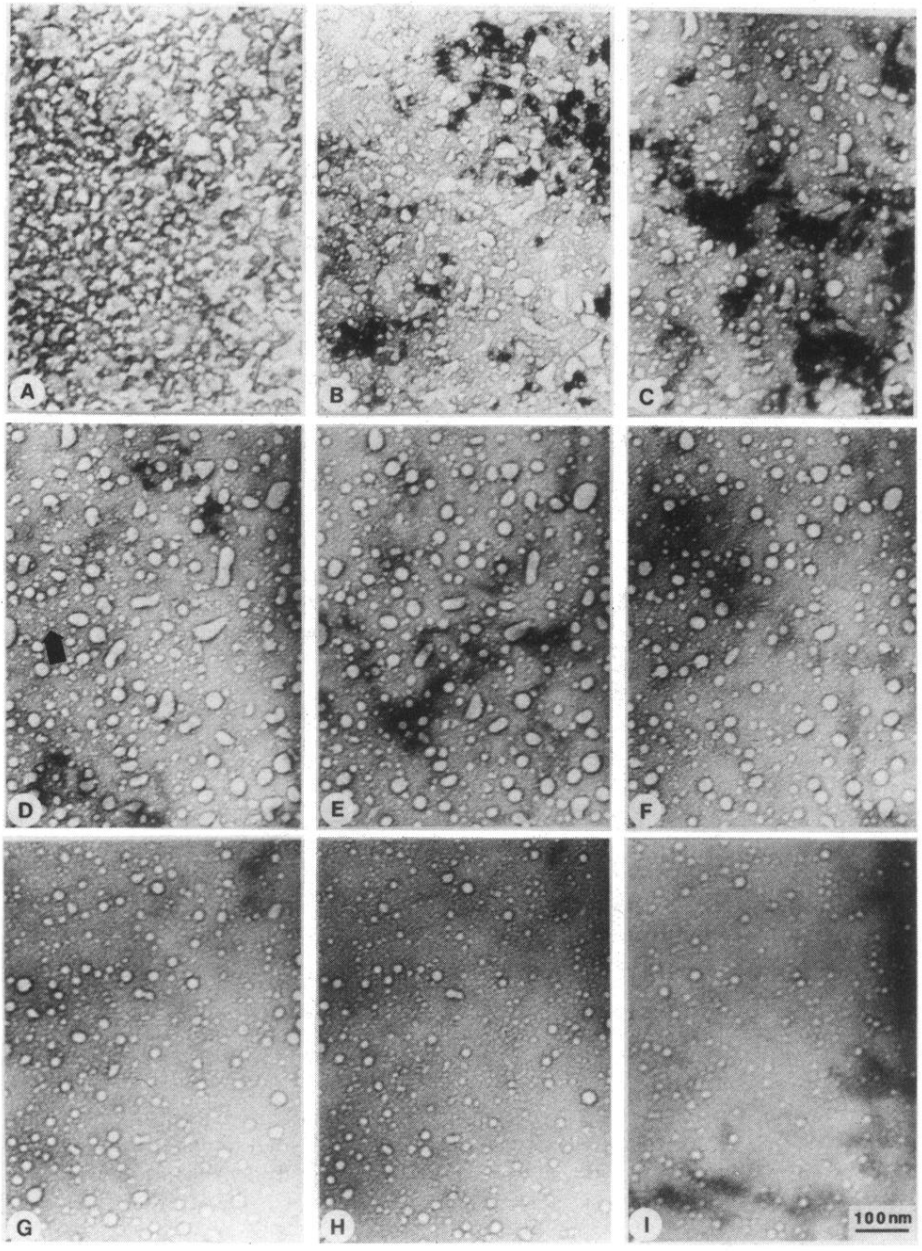

FIG. 1. TEM micrographs showing He bubble evolution during 200-keV Xe irradiation at room temperature. Xe dose of (a) 0, (b) 2, (c) 4, (d) 6, (e) 8, (f) 10, (g) 12, (h) 13, and (i) 15×10^{15} Xe/cm^2.

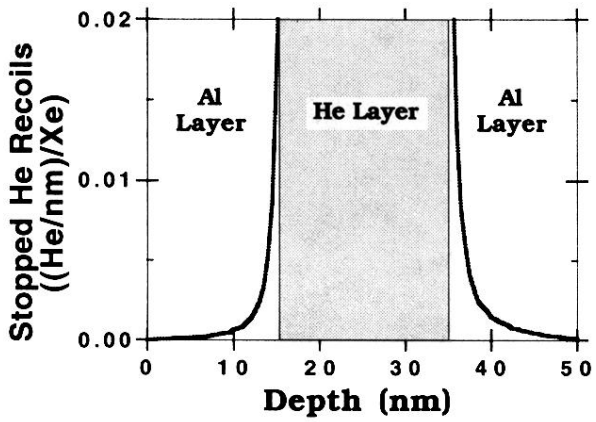

FIG. 5. Results of TRIM calculations of stopping of He ejected from a 20-nm-thick He layer containing 2.5×10^{21} He/cm^3 sandwiched between 15-nm-thick layers of Al. 200-keV Xe ions were incident from the left.